Communication

W-band orientation selective DEER measurements on a Gd^{3+}/nitroxide mixed-labeled protein dimer with a dual mode cavity

Ilia Kaminker [a,1], Igor Tkach [b,1], Nurit Manukovsky [a], Thomas Huber [c], Hiromasa Yagi [c], Gottfried Otting [c], Marina Bennati [b,*], Daniella Goldfarb [a,*]

[a] Department of Chemical Physics, Weizmann Institute of Science, Rehovot, Israel
[b] Max Planck Institute for Biophysical Chemistry and Department of Chemistry, University of Göttingen, Göttingen, Germany
[c] Research School of Chemistry, Australian National University, Canberra, ACT 0200, Australia

ABSTRACT

Double electron–electron resonance (DEER) at W-band (95 GHz) was applied to measure the distance between a pair of nitroxide and Gd^{3+} chelate spin labels, about 6 nm apart, in a homodimer of the protein ERp29. While high-field DEER measurements on systems with such mixed labels can be highly attractive in terms of sensitivity and the potential to access long distances, a major difficulty arises from the large frequency spacing (about 700 MHz) between the narrow, intense signal of the Gd^{3+} central transition and the nitroxide signal. This is particularly problematic when using standard single-mode cavities. Here we show that a novel dual-mode cavity that matches this large frequency separation dramatically increases the sensitivity of DEER measurements, allowing evolution times as long as 12 μs in a protein. This opens the possibility of accessing distances of 8 nm and longer. In addition, orientation selection can be resolved and analyzed, thus providing additional structural information. In the case of W-band DEER on a Gd^{3+}–nitroxide pair, only two angles and their distributions have to be determined, which is a much simpler problem to solve than the five angles and their distributions associated with two nitroxide spin labels.

© 2012 Elsevier Inc. All rights reserved.

1. Introduction

The pulse DEER (double electron–electron resonance) experiment [1–3], also known as PELDOR (Pulsed Electron Double Resonance), has become very popular in recent years for measuring nanometer range distances in biological macromolecules for structural biology applications [4,5]. The most common application of DEER is to measure distances between two nitroxide spin labels (SLs) attached at specific points in the macromolecules of interest. Effective methods to attach nitroxide SLs to both proteins [6] and nucleic acids [7,8] have been developed and applied extensively. These measurements are most commonly carried out at X-band (~9.5 GHz, ~0.35 T) and less frequently at Q-band frequencies (~34 GHz, 1.3 T) frequencies [9]. While the intrinsic sensitivity of DEER measurements is greatly enhanced at W-band, such measurements exhibit extensive orientation selection. This occurs when the orientations of the two paramagnetic centers are correlated, and when not all possible orientations of the interspin vector with respect to the magnetic field contribute to the DEER trace

[10]. This is because the *g*-anisotropy of organic radicals, and particularly nitroxide SLs, is resolved at W-band frequencies, which, together with the limited bandwidth of the microwave pulses, leads to orientation-selection effects in the DEER traces [10–17]. Accordingly, the DEER traces depend not only on the inter-electron distance but also on a set of five additional angles and their distributions. The angular dependence can be described by three Euler angles defining the relative orientation of the *g*-tensors of the two nitroxides and a polar and an azimuthal angle describing the orientation of the inter-electron vector relative to one of the *g*-tensors. This rather large number of parameters turns the analysis of W-band DEER data into a difficult task, in particular for partially flexible systems.

To circumvent this difficulty, without having to compromise on the high sensitivity offered by high fields, a new class of SLs based on Gd^{3+} chelates has recently been proposed and implemented at W- and Q-band [12,18–22]. The high-spin Gd^{3+} ($S = 7/2$) SLs were shown to behave similar to spin ½ SLs in DEER measurements, allowing the use of well-established data analysis software developed for the $S = 1/2$ case [23]. Utilizing Gd^{3+} based SLs, distance measurements of up to about 6 nm were recently reported for both a DNA duplex [21] and a protein homodimer [22]. An alternative approach could involve the use of a trityl radical-derived spin label, which has a practically isotropic *g*-tensor, as recently demonstrated by Hubbell and Freed [24]. They were able to perform a dis-

tance measurement using the double-quantum coherence (DQC) experiment at 17 GHz and, remarkably, could perform the measurements at room temperature following immobilization of the protein on a matrix, albeit only for a short distance.

The pair-wise time evolution of the echo intensity in a DEER experiment is given by [2,3]:

$$V(t) = V_0(1 - \lambda(1 - \cos \omega_{dd}(1 - 3\cos^2 \theta_{dd})t)) \tag{1}$$

where

$$\omega_{dd} = \frac{g_1 g_2 \beta^2 \mu_0}{4\pi \bar{h} r^3}$$

V_0 is the echo intensity at the time $t = 0$, g_1 and g_2 are the g values of the two spins, r is the inter-electron distance, θ_{dd} is the angle between the inter-electron vector, r, and the magnetic field, β is the Bohr magneton, μ_0 is the magnetic permeability of vacuum, and $\bar{h}$ is Planck's constant. λ is the so-called modulation depth parameter which represents the fraction of the spins affected by the pump pulse. Under conditions of orientation selection λ becomes orientation dependent. In general, the signal-to-noise ratio of DEER is given by [4,25]

$$S/N \propto \lambda V_0 e^{-2t_{max}/T_M} \left(\sqrt{T_1}\right)^{-1} \tag{2}$$

where t_{max} is the maximum DEER evolution time (see Fig. 1a), and T_M and T_1 are, respectively, the phase-memory and the spin–lattice relaxation times of the observed spins. Eq. (2) neglects the contribution of the background decay. A major drawback of Gd^{3+}–Gd^{3+} DEER measurements is the relatively small size of λ, arising from the broad spectrum of all transitions with the exception of the central $|-1/2\rangle \rightarrow |1/2\rangle$ transition [18,20,22]. At high magnetic fields, this is compensated by a large V_0 value and a relatively short T_1 time. A further increase in S/N ratio, however, can be gained by using mixed spin labels, namely Gd^{3+} as the observed spins and nitroxide as the pump spins. The nitroxide is chosen as pump spins because of

its narrower spectrum, which results in a higher λ value. Moreover, it has a longer T_1 time, ($\sim$100 ms as opposed to $\sim$100 μs for Gd^{3+} complexes) which makes it unfavorable as observed spin. In the DEER experiment only the observer spins need to recover to thermal equilibrium, and therefore it is their T_1 that has to be taken into account when adjusting the repetition rate. In such a spin pair, however, orientation selection is reintroduced. Nonetheless, the situation is simplified by the isotropic character of the Gd^{3+} spectrum, requiring only two angles, the polar and azimuthal angles θ and ϕ that define the orientation of r relative to the principal g-frame of the nitroxide. A similar situation is encountered in a mixed trityl-nitroxide pair reported recently [26].

The potential of DEER distance measurements between a nitroxide SL and a Gd^{3+} ion was first demonstrated on a model compound with a rigid spacer and a Gd^{3+}–nitroxide distance of $\sim$2.5 nm, using X-band and Q-band spectrometers [27]. This was followed by W-band DEER distance measurements on a protein dimer, a mutant of the ERp29 chaperon [28]. The sample contained a statistical distribution of dimers labeled with Gd^{3+}–nitroxide (50%), Gd^{3+}–Gd^{3+} (25%) and nitroxide–nitroxide (25%) (Fig. 1b). By exploiting the different spectroscopic properties of the two types of labels, it was possible to select the Gd^{3+}–Gd^{3+}, nitroxide–Gd^{3+}, and nitroxide–nitroxide distance distributions, in the range of 6 nm, using a very small quantity of protein (about 0.3 nmol in total). A similar approach was applied to nano-sized gold particles functionalised with nitroxide radicals and Gd^{3+}–DTPA complexes at X- and Q-band [29].

At W-band the frequency spacing between the Gd^{3+} central transition and the nitroxide most intense signal is $\sim$700 MHz because of their different g-values. This exceeds by far the bandwidth of the standard cylindrical cavities commonly used in W-band spectrometers. Accordingly, the previously reported W-band Gd^{3+}–nitroxide DEER measurements were carried out under conditions far from optimal [28]. The frequency separation used was 65 MHz and the observe pulse was set to the broad background
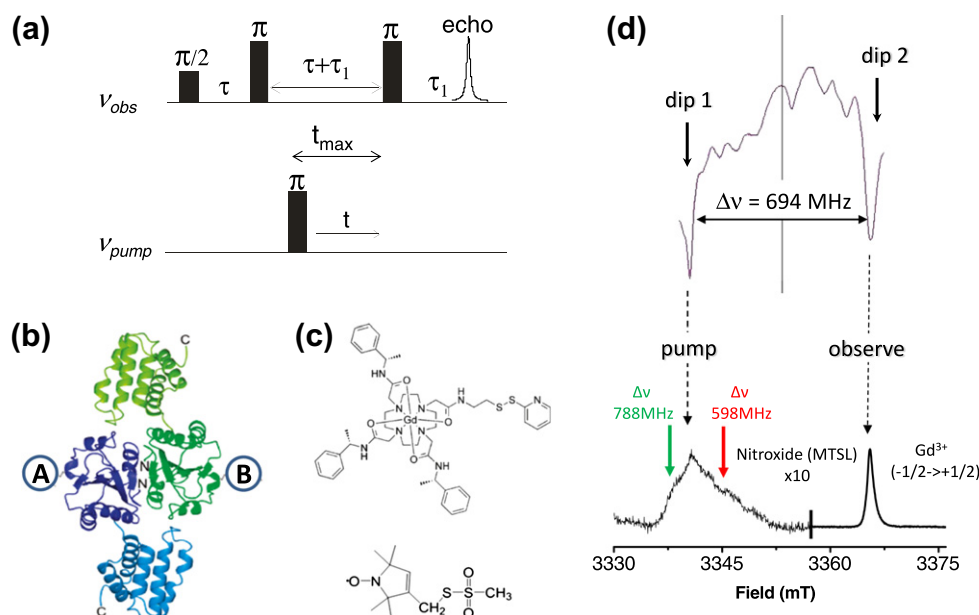

Fig. 1. Experimental setup. (a) 4-pulse DEER pulse sequence used. (b) Structure of the ERp29 protein dimer (PDB ID 2QC7) [33]. The spin labeling positions (S114C) are identified by circles. (c) The Gd^{3+} C1 tag (top) and MTSL tag (bottom) used to spin-label the protein. (d) Characteristic tuning curve showing the two modes of the resonator separated by 694 MHz. This setup was used to apply the pump pulse at the frequency of the g_y component of the nitroxide spectrum. The modes excited in the resonator are TE_{012} (dip 1) and TE_{012}-ϕ_0 (dip 2). The subscript "-ϕ_0" of the second mode indicates the "zero" phase shift between fields in the neighboring resonance cells of the resonator. The mode is a combination of two cylindrical TE_{011} half-wave alternations oscillating in phase in two different cells. The echo-detected EPR spectrum of the statistically labeled ERp29 protein dimer is shown below. Experimental parameters: MW frequency 93.7 GHz; $\pi/2$ and π pulse durations of 40 ns and 80 ns, respectively; τ = 284 ns; T = 10 K; repetition time 11 ms. Different phase corrections were needed in the two parts of the spectrum to represent both the nitroxide and Gd^{3+} spectrum as absorption lines. All experiments were performed on a Bruker ElexSys E 680 spectrometer (MPIbpc, Göttingen) (see Section 4).

of the "other" transitions of the Gd^{3+}, thus considerably reducing V_0. The small frequency separation also leads to severe direct off-resonance effects of the pump pulse (optimized for $S = \frac{1}{2}$) on the observe echo of the $S = 7/2$ ion, decreasing V_0 even further.

In this work we demonstrate the full potential of nitroxide-Gd^{3+} high-field (W-band) DEER distance measurements using a novel dual-mode cavity [30,31] that allows a frequency separation of 700 MHz and more. This is demonstrated with the 51 kDa homodimer of the ERp29 chaperone studied previously [28]. The considerable improvement in S/N achieved under the new, much more favorable conditions allowed evolution times as long as 12 μs, which make distances of 8 nm easily accessible. In addition, orientation selection could be resolved and analyzed.

2. Results and discussion

For the present set of experiments, we used two preparations of the ERp29 S114C/C157S double-mutant, one labeled with a C1-Gd^{3+} tag [32] and the other with the MTSL nitroxide spin label. Mixing and incubation resulted in mixed dimers as described previously (Fig. 1b and c) [28]. Fig. 1d shows the echo-detected EPR spectrum of this sample, recorded under conditions optimized for nitroxide observation, along with the frequency response of the dual mode cavity. It shows how the two frequency-dips were adjusted to coincide with the maximum signal of the Gd^{3+} and the nitroxide.

Three DEER traces with the pump pulse set to the g_x ($\Delta v = 788$ MHz), g_y ($\Delta v = 694$ MHz), and g_z ($\Delta v = 598$ MHz) components of the nitroxide spectrum and the observe pulse set to the Gd^{3+} central transition are shown in Fig. 2a and the corresponding Fourier transforms (FTs) are shown in Fig. 2b. The DEER traces prior to background removal are depicted in Fig. S1 in the Supplementary Information (SI). Fig. 2 also displays the sum of the three traces and the corresponding FT. Since the spectrum of the observer spins (Gd^{3+}) is essentially isotropic because of the narrow central transition and the distribution in the ZFS parameters, in order to obtain full dipolar Pake pattern it is sufficient to sum several DEER traces with the pump pulse applied to different positions that together cover the whole nitroxide EPR spectrum. In our case summing three DEER traces with the pump pulse applied at g_x, g_y and g_z seemed sufficient. This, however, may be a consequence of the large distribution present. This issue should be looked into in more details as the number of DEER traces are likely to depend on the width of the distance distribution. The FT-DEER spectra clearly demonstrate orientation dependence. Singularities corresponding to $\theta_{dd} = 0$, at ±0.48 MHz, are particularly obvious in the FT-DEER

traces acquired with the pump pulse set to the g_x positions, while the other two primarily show singularities corresponding to $\theta_{dd} = 90°$, at ±0.24 MHz. From these two features, we deduced an inter-electron distance of 5.75 nm, which is in good agreement with the previously reported value [28].

The observed significant degree of orientation selection is consistent with the CW nitroxide spectrum that reveals a significant degree of motional restriction (Fig. S1 in Ref. [28]). As expected, the DEER trace collected with the pump pulse set to g_y position displays the smallest degree of orientation selection. Indeed, its FT-DEER spectrum looks like a Pake pattern and is close to that obtained from the sum of the DEER traces (Fig. 2b). It can be seen that the dual mode cavity allowed the collection of DEER data up to 12 μs evolution time, as compared to 5 μs in a traditional cylindrical cavity. This difference is remarkable as it indicates that distances as long as 8 nm or even greater are easily accessible with this setup for Gd^{3+}–nitroxide pairs.

In our earlier work we reported that the application of the pump pulse on the nitroxide caused a considerable reduction of the echo intensity of the observed Gd^{3+} signal [28]. We showed that this echo reduction mostly originated from off-resonance irradiation effects and that increasing the separation between the observer and pump pulses could substantially reduce this problem. Indeed, this effect was marginal with the current setup. The echo reduction phenomenon was also reported for Gd^{3+}–nitroxide distances carried out at X- and Q-band with single-mode cavities and was analyzed using full density matrix simulations based on full matrix diagonalization of a $S = 1/2$, $S = 7/2$ system [29].

A further significant increase in sensitivity is possible, as in our experiments the pump pulse was set to 64 ns because of power limitations (see Section 4). Using higher mw power [14,34] it would be possible to invert a wider range of the pumped spins thus increasing λ. The estimated Q values of the loaded cavity at 10 K were approximately 3000 and 1800, for TE_{012} and TE_{012}-ϕ_0 modes, which correspond to bandwidths of approximately 31 and 52 MHz for the pump and observer frequencies, respectively. The nitroxide pump pulse, 56–64 ns was applied at the TE_{012} mode. The length of these pulses can be further reduced by a factor of ~2 before running into bandwidth limitations. This would require a mw power increase by a factor of 4 (>1.6 W instead of 400 mW). In contrast, for the observe pulses of 14–16 ns, applied to the Gd^{3+}, a power increase will probably not lead to a significant sensitivity improvement due to resonator bandwidth limitations.

An additional increase in S/N can be obtained by increasing the repetition rate. In the present situation the repetition rate was
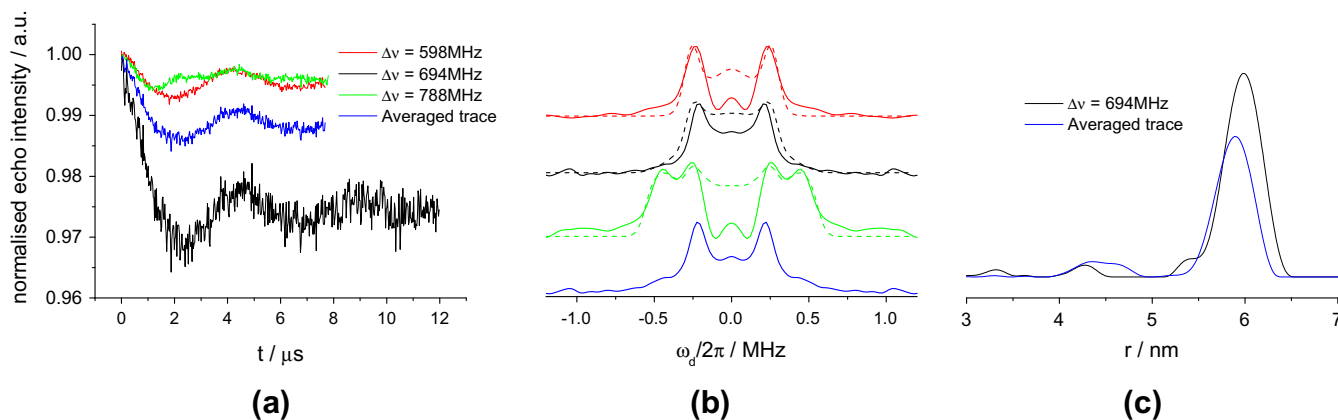

Fig. 2. DEER measurements on mixed labeled ERp29 dimers at 10 K. (a) Time domain traces after background removal (raw data shown in Fig. S1). (b) Their corresponding Fourier transforms (solid lines). Best-fit simulations are shown as dashed lines. (c) Distance distribution obtained with the regularization parameter $\alpha = 100$ using DeerAnalysis [23]. The experimental parameters are given in the main text. (For interpretation of the references to color in this figure, the reader is referred to the web version of this article.)

determined by instrumental constrains and not the Gd^{3+} spin lattice relaxation.

The resolved orientation selection shown in Fig. 2 allowed us to obtain the relative orientation of r with respect to the principal axis system of the nitroxide g-tensor, which is determined by the angles θ, ϕ, and their distributions. This was achieved by carrying out best-fit simulations of the three FT-DEER spectra shown in Fig. 2b. The details of the simulations are described in the SI and the best fit was determined by least squares searching over the range spanned by θ, ϕ, and their distributions for a given distance distribution. In general, we followed the approach described in [13] with the modification that the orientation selection arises from only the pumped spins and taking into account the rhombicity of g that is well resolved at W-band. The parameters r, θ and ϕ were assumed to be uncorrelated, each having a Gaussian distribution. The best-fit and experimental spectra are compared in Fig. 2b. Our best-fit procedure considered only the regions from ±0.12 MHz to ±0.6 MHz. We did not consider the center of the spectrum in the best-fit simulations due to its high sensitivity to the variation in the removal of the background decay. Similarly, we omitted the wings of the spectra at frequencies higher than ±0.6 MHz, since they reflect spurious short distances (see the distances in the range of 2–4 nm in Fig. 2c), which most probably result from limited S/N. The best fit simulations gave $\theta = 90°$ and $\phi = 180°$ with widths of the respective Gaussian distributions of $\Delta\theta = 10°$ and $\Delta\phi = 110°$. The distributions obtained from the best-fit simulation are shown in Fig. 3a.

We also calculated the most probable distributions of θ and ϕ based on the structure of ERp29 and all possible conformations of the C1 and MTSL tags, as shown in Fig. 3b (see the SI for details). Such a calculation yields for each combination of the conformation of the two tags a set of r, θ and ϕ. To allow comparison with the values obtained for θ and ϕ, their individual probability distributions were calculated. The calculation shows a broad range of orientations, reflecting the flexibility of the two tags, with the highest probability for $\theta = 90°$ and $\phi = 180°$. The labeling site S114C is located before the third β-strand in the N-terminal domain of ERp29. While the position is solvent exposed and allows ready access of the labeling reagent, residues 110–117 neighboring in the primary sequence as well as residues D61, P131, Y132 and T133 are in close spatial proximity (less than 0.8 nm) restricting mobility of the MTSL spin label (an example of one rotamer is shown in Fig. S3). This is in good agreement with our experimental results. It is important to note that the intrinsic symmetry of the second-rank tensors prevents the distinction between $\phi = 0°$ and $\phi = 180°$ based on the simulations alone. While the calculations show some

significant contributions in the range of $\theta = 30–60°$ these were not found experimentally. Simulations carried out with the calculated θ and ϕ distribution (not shown) gave a g_x dipolar spectrum with significantly reduced $\theta_{dd} = 0°$ features compared to the experimental spectrum. The essential assumption that makes the analysis of the experimental data possible is that the interspin distance r, and the θ and ϕ angles are uncorrelated. This is of course a rather coarse assumption since the reorientation of the nitroxide tether will result in a simultaneous, correlated, change in all three parameters, namely each conformation has specific r, and the θ and ϕ. To account for this in spectral simulations is practically impossible. In addition, three independent parameters with their respective distributions cover a large parameter space so further simplifications are needed in order to make the fitting procedure feasible. In this case, apart from being uncorrelated, we assumed that all parameters are distributed normally. It seems that recovering the shape of the distribution for any of the parameters from the data available will not give any unique results and is practically impossible. This simplification may account for the difference in the distributions in ϕ, that although broad, is different than Gaussian. The difference in the distribution in θ is however more significant, and indicates that some of the conformations found in the simulations are not found experimentally. The reason for this is currently not clear but the experimental data clearly show a high preference for r being in the xy plane.

Finally, in the particular case discussed in this article, the orientation selection was very clear and from the experimental data it was easy to recognize that the $\theta_{dd} = 0$ (or 180°) features are strongest along g_x, giving a clear indication to the direction of r. Other cases, however, are not expected to be more complicated, as one has to look for the g-value at which the $\theta_{dd} = 0$ features are the strongest and get a good estimation for θ.

3. Conclusions

The potential of W-band DEER distance measurements on mixed Gd^{3+}–nitroxide labeled samples using a dual-mode cavity was demonstrated on a protein with a Gd^{3+}–nitroxide distance close to 6 nm, using an effective concentration of 50 μM and a volume of 2–3 μl. The dramatic improvement in S/N afforded by the dual-mode cavity allowed acquiring data up to 12 μs evolution time, which highlights the potential of the method to access distances of 8 nm and above. Orientation selection could be resolved and analyzed, thus providing additional structural information. In the case of W-band DEER on Gd^{3+}–nitroxide pairs, only two angles
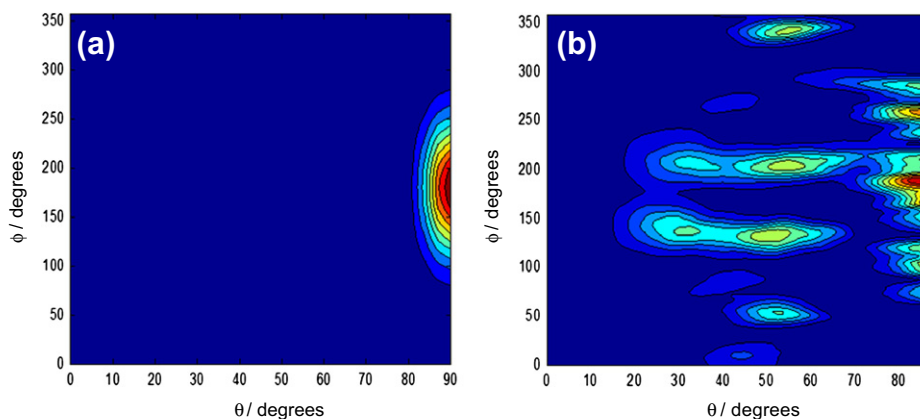

Fig. 3. Probability distribution of θ and ϕ angles that define the orientation of the interspin vector r in the g – principal axis system for different nitroxide conformers as obtained from (a) fitting of the experimental dipolar spectra and (b) molecular modeling. See text for details. Color scale: Red – most probable; blue – least probable. (For interpretation of the references to color in this figure legend, the reader is referred to the web version of this article.)

and their distributions have to be determined for accurate distance measurements, which is considerably simpler to achieve compared to the five angles and their distributions needed for distance measurements between two nitroxide labels at this frequency. Labeling a monomeric protein with both a Gd^{3+} binding tag and MTSL requires extra synthetic efforts like the use of unnatural amino-acids [35] and this may prevent such routine applications. In contrast, the application of such types of mixed labeling is straightforward for studying complexes of two proteins, or protein-DNA, where each molecule is labeled with a different label using standard methods.

4. Experimental details

To set the optimal frequency separation for the DEER experiments, we employed a dual-mode cavity, which supports two cylindrical microwave modes at the position of the sample and allows tuning of their frequency separation in a broad range [30,31]. The bimodal cavity is implemented into a probe head adapted for the operation with a commercial Bruker E 680 Elexsys W-band spectrometer. The spectrometer is equipped with the Power Upgrade Module II (Bruker) providing 400 mW microwave power at the output of the bridge. In this set up, the resonator achieves a typical $\pi/2$ pulse length of about 36–40 ns for nitroxide radicals. Precise tuning of the frequency separation up to ~700 MHz was achieved by using the standard frequency sweeper implemented in the Bruker bridge with a sweeping range of up to 740 MHz. The screenshot of the tuning picture for the separation of the dips by about 700 MHz is displayed in Fig. 1d. Tuning for a higher frequency separation range (>700 MHz) was impeded by the restricted range of the sweeper. The quality factor of the dips was not impaired by the large frequency separation, as evidenced by the Rabi nutations at both frequencies, which corresponded to $\pi/2$ pulse lengths of 36 ns and 16 ns for the nitroxide and Gd^{3+}, respectively. Since the Q-factor of the higher frequency mode (TE_{012}), which was applied to pump the nitroxide, is inherently higher, the ratio of the pulse lengths applied to different labels does not exactly match the ratio of the related transition probabilities.

All experiments were performed at 10 K using the standard four-pulse DEER sequence [3] (Fig. 1a). To set the proper frequency separation, electron spin echo-detected EPR spectra were recorded prior to the DEER experiments, using the optimized pulse lengths for the Gd^{3+} and nitroxide, respectively. The optimal lengths for the pump and detection pulses were verified by echo nutation experiments. The DEER experiments were performed by setting the "observer" frequency at the maximum of the most intense line ($|-1/2\rangle \rightarrow |1/2\rangle$ transition) of the Gd^{3+} and by varying the "pump" frequency over the spectral range of the nitroxide radical.

The typical DEER experimental conditions were: $\Delta\nu_{pump-observe}$ = 598–798 MHz, τ = 380 ns, $t_{\pi/2}$ (observe) = 14–16 ns, t_{π}(pump) = 56–64 ns, and a repetition rate of 1 kHz. In principle, higher acquisition rates were possible for the system under study, by decreasing the repetition time of the experiment down to 100–200 μs as appropriate for Gd^{3+} observer spins but such high repletion rates were prevented by the spectrometer hardware. Thus, the measurement time was prolonged by the restricted sequence repetition rate possible on the spectrometer. The typical number of averaged scans was in the range of 150–800 depending on the echo time evolution gate (6.3–12.3 μs) and the position of the pumping pulse, corresponding to total recording times of approximately 1–5 h at the 1 kHz repetition rate. When exciting exactly at the g_y position of the nitroxide spectrum, however, DEER traces with acceptable S/N could be recorded in just a few minutes (~9 min, 20 scans, 6.3 μs evolution gate). The dipolar evolution time was varied in different experiments. A two-step phase cycle was applied to compensate for DC offsets.

Appendix A. Supplementary material

Supplementary data associated with this article can be found, in the online version, at http://dx.doi.org/10.1016/j.jmr.2012.11.028.

References

[1] R.G. Larsen, D.J. Singel, Double electron electron resonance spin echo modulation – spectroscopic measurements of electron-spin pair separations in orientationally disordered solids, J. Chem. Phys. 98 (1993) 5134–5146.

[2] A.D. Milov, A.B. Ponomarev, Y.D. Tsvetkov, Electron electron double-resonance in electron spin echo – model biradical systems and the sensitized photolysis of decalin, Chem. Phys. Lett. 110 (1984) 67–72.

[3] M. Pannier, S. Veit, A. Godt, G. Jeschke, H.W. Spiess, Dead-time free measurement of dipole–dipole interactions between electron spins, J. Magn. Reson. 142 (2000) 331–340.

[4] P.P. Borbat, J.H. Freed, Measuring distances by pulsed dipolar ESR spectroscopy: spin-labeled histidine kinases, Methods Enzymol. 423 (2007) 52–116.

[5] O. Schiemann, T.F. Prisner, Long-range distance determinations in biomacromolecules by EPR spectroscopy, Q. Rev. Biophys. 40 (2007) 1–53.

[6] W.L. Hubbell, A. Gross, R. Langen, M.A. Lietzow, Recent advances in site-directed spin labeling of proteins, Curr. Opin. Struct. Biol. 8 (1998) 649–656.

[7] X.J. Zhang, P. Cekan, S.T. Sigurdsson, P.Z. Qin, Studying RNA using site-directed spin-labeling and continuous-wave electron paramagnetic resonance spectroscopy, Methods Enzymol. 469 (2009) 303–328.

[8] G. Sicoli, F. Wachovious, M. Bennati, C. Höbartner, Probing secondary structures of spin-labeled RNA by pulse EPR spectroscopy, Angew. Chem. Int. Ed. 49 (2010) 1–6.

[9] P. Zou, H.S. McHaourab, Increased sensitivity and extended range of distance measurements in spin-labeled membrane proteins: Q-band double electron–electron resonance and nanoscale bilayers, Biophys. J. 98 (2010) L18–L20.

[10] V.P. Denysenkov, T.F. Prisner, J. Stubbe, M. Bennati, High-field pulsed electron-electron double resonance spectroscopy to determine the orientation of the tyrosyl radicals in ribonucleotide reductase, Proc. Natl. Acad. Sci. U. S. A. 103 (2006) 13386–13390.

[11] Y. Polyhach, A. Godt, C. Bauer, G. Jeschke, Spin pair geometry revealed by high-field DEER in the presence of conformational distributions, J. Magn. Reson. 185 (2007) 118–129.

[12] A. Potapov, H. Yagi, T. Huber, S. Jergic, N.E. Dixon, G. Otting, D. Goldfarb, Nanometer-scale distance measurements in proteins using Gd^{3+} spin labeling, J. Am. Chem. Soc. 132 (2010) 9040–9048.

[13] C. Abe, D. Klose, F. Dietrich, W.H. Ziegler, Y. Polyhach, G. Jeschke, H.-J. Steinhoff, Orientation selective DEER measurements on vinculin tail at X-band frequencies reveal spin label orientations, J. Magn. Reson. 216 (2012) 53–61.

[14] G.W. Reginsson, R.I. Hunter, P.A.S. Cruickshank, D.R. Bolton, S.T. Sigurdsson, G.M. Smith, O. Schiemann, W-band PELDOR with 1 kW microwave power: molecular geometry, flexibility and exchange coupling, J. Magn. Reson. 216 (2012) 175–182.

[15] A. Savitsky, A.A. Dubinskii, H. Zimmermann, W. Lubitz, K. Möbius, High-field dipolar electron paramagnetic resonance (EPR) spectroscopy of nitroxide biradicals for determining three-dimensional structures of biomacromolecules in disordered solids, J. Phys. Chem. B 115 (2011) 11950–11963.

[16] J.E. Lovett, A.M. Bowen, C.R. Timmel, M.W. Jones, J.R. Dilworth, D. Caprotti, S.G. Bell, L.L. Wong, J. Harmer, Structural information from orientationally selective DEER measurements, Phys. Chem. Chem. Phys. 11 (2009) 6840–6848.

[17] V.P. Denysenkov, D. Biglino, W. Lubitz, T.F. Prisner, M. Bennati, Structure of the tyrosyl biradical in mouse R2 ribonucleotide reductase from high-field PELDOR, Angew. Chem. Int. Ed. 47 (2008) 1224–1227.

[18] M. Gordon, I. Grossman, Y. Kaminker, Gofman, Y. Shai, D. Goldfarb, W-band pulse EPR distance measurements in peptides using Gd^{3+}-dipicolinic acid derivatives as spin labels, Phys. Chem. Chem. Phys. 22 (2011) 10771–10780.

[19] A. Potapov, Y. Song, T.J. Meade, D. Goldfarb, A.V. Astashkin, A. Raitsimring, Distance measurements in model bis-Gd(III) complexes with flexible "bridge". Emulation of biological molecules having flexible structure with Gd(III) labels attached, J. Magn. Reson. 205 (2010) 38–49.

[20] A.M. Raitsimring, C. Gunanathan, A. Potapov, I. Efremenko, J.M.L. Martin, D. Milstein, D. Goldfarb, Gd^{3+} complexes as potential spin labels for high field pulsed EPR distance measurements, J. Am. Chem. Soc. 129 (2007) 14138–14140.

[21] Y. Song, T.J. Meade, A.V. Astashkin, E.L. Klein, J.H. Enemark, A. Raitsimring, Pulsed dipolar spectroscopy distance measurements in biomacromolecules labeled with Gd(III) markers, J. Magn. Reson. 210 (2011) 59–68.

[22] H. Yagi, D. Banerjee, B. Graham, T. Huber, D. Goldfarb, G. Otting, Gadolinium tagging for high-precision measurements of 6 nm distances in protein assemblies by EPR, J. Am. Chem. Soc. 133 (2011) 10418–10421.

[23] G. Jeschke, V. Chechik, P. Ionita, A. Godt, H. Zimmermann, J. Banham, C.R. Timmel, D. Hilger, H. Jung, DeerAnalysis2006 – a comprehensive software package for analyzing pulsed ELDOR data, Appl. Magn. Reson. 30 (2006) 473–498.

[24] Z. Yang, Y. Liu, P. Borbat, J.L. Zweier, J.H. Freed, WS.L. Hubbell, Pulsed ESR dipolar spectroscopy for distance measurements in immobilized spin labeled proteins in liquid solution, J. Am. Chem. Soc. 134 (2012) 9950–9952.

[25] P.P. Borbat, J.H. Freed, in: G.R.E.L.J. Berliner, S.S. Eaton (Eds.), Biol. Magn. Reson, vol. 19, Kluwer, Academic, NY, 2000, pp. 383–459.

[26] G.W. Reginsson, N.C. Kunjir, S.T. Sigurdsson, O. Schiemann, Trityl radicals: spin labels for nanometer-distance measurements, Chem. – Eur. J. 18 (2012) 13580–13584.

[27] P. Lueders, G. Jeschke, M. Yulikov, Double electron–electron resonance measured between $Gd^{(3+)}$ ions and nitroxide radicals, J. Phys. Chem. Lett. 2 (2011) 604–609.

[28] I. Kaminker, H. Yagi, T. Huber, A. Feintuch, G. Otting, D. Goldfarb, Spectroscopic selection of distance measurements in a protein dimer with mixed nitroxide and Gd^{3+} spin labels, Phys. Chem. Chem. Phys. 14 (2012) 4355–4358.

[29] M. Yulikov, P. Lueders, M.F. Warsi, V. Chechik, G. Jeschke, Distance measurements in Au nanoparticles functionalized with nitroxide radicals and Gd^{3+}–DTPA chelate complexes, Phys. Chem. Chem. Phys. 14 (2012) 10732–10746.

[30] I. Tkach, G. Sicoli, C. Höbartner, M. Bennati, A dual-mode microwave resonator for double electron–electron spin resonance spectroscopy at W-band microwave frequencies, J. Magn. Reson. 209 (2011) 341–346.

[31] I. Tkach, M. Bennati, Dual-Mode Microwave Resonator Device and Method of Electron Spin Resonance Measurement, Int. PA publication Nr. WO2012/013202, European PA Publication Nr. EP 2486416 A1.

[32] B. Graham, C.T. Loh, J.D. Swarbrick, P. Ung, J. Shin, H. Yagi, X. Jia, S. Chhabra, G. Pintacuda, T. Huber, G. Otting, Bioconjugate Chem. 22 (2011) 2118–2125.

[33] N.N. Barak, P. Neumann, M. Sevvana, M. Schutkowski, K. Naumann, M. Malesevic, H. Reichardt, G. Fischer, M.T. Stubbs, D.M. Ferrari, Crystal structure and functional analysis of the protein disulfide isomerase-related protein ERp29, J. Mol. Biol. 385 (2009) 1630–1642.

[34] D. Goldfarb, Y. Lipkin, A. Potapov, Y. Gorodetsky, B. Epel, A.M. Raitsimring, M. Radoul, I. Kaminker, HYSCORE and DEER with an upgraded 95 GHz pulse EPR spectrometer, J. Magn. Reson. 194 (2008) 8–15.

[35] M.R. Fleissner, E.M. Brustad, T. Kálai, C. Altenbach, D. Cascio, F.B. Peters, K. Hideg, S. Peuker, P.G. Schultz, W.L. Hubbell, Site-directed spin labeling of a genetically encoded unnatural amino acid, Proc. Natl. Acad. Sci. U. S. A. 106 (2009) 21637–21642.